MtvS Regulates the *Francisella* Type V-A CRISPR-Cas System

Maj Brodmann and Luciano A. Marraffini*

Laboratory of Bacteriology, The Rockefeller University, New York, NY 10065, USA

* Howard Hughes Medical Institute, The Rockefeller University, New York, NY 10065, USA

Correspondence: mbrodmann@rockefeller.edu, marraffini@rockefeller.edu

Abstract

CRISPR-Cas systems endow bacteria and archaea with adaptive immune systems against mobile genetic elements, playing a fundamental role in shaping microbial communities. Many organisms harbor more than one CRISPR-Cas system, however whether and how these are differentially regulated is not known, in many instances due to the impossibility of studying CRISPR immunity in native hosts. Here we studied the regulation of endogenous type II-B and type V-A CRISPR-Cas systems in opportunistic human pathogen *Francisella novicida* U112. Fluorescence microscopy and transcriptomics experiments revealed that while the type II-B system is constitutively expressed, the type V-A CRISPR-Cas system is differentially expressed at stationary phase and high cell density. Using mass spectrometry and genetics we identified MtvS as a factor required for the differential expression of the type V-A CRISPR-Cas locus. Surprisingly, MtvS-dependent expression of the type V-A CRISPR-Cas system at high cell density is linked quorum sensing like behavior, even though *F. novicida* U112 lacks canonical quorum sensing genes. Our findings provide an example of how bacteria harboring multiple CRISPR systems regulate their expression.

Introduction

CRISPR (Clustered regularly short interspaced palindromic repeats)-Cas (CRISPR associated genes) systems protect bacteria and archaea against foreign nucleic acids such as phages and genetic mobile elements[1,2]. CRISPR-Cas systems are adaptive immune systems that can store memories of previous infections in the form of short invader-derived sequences that are inserted in between the repeats of the CRISPR array during infection[3–5]. CRISPR arrays are transcribed into cr(CRISPR)RNAs that guide Cas effectors to complementary sequences on the invading foreign elements[6,7] and destroy them [8–13]. Prokaryotic organisms often encode multiple CRISPR-Cas loci, which may be differently regulated[14]. Previous studies have reported Cas proteins, crRNAs, transcriptional regulators, quorum sensing and two component signaling systems involved in the regulation CRISPR-Cas systems [15–35]. Detailed investigation of regulatory networks governing CRISPR expression, however, has been difficult due to the lack of natural hosts that can be used as experimental systems for CRISPR-Cas immunity.

Here we studied the endogenous type II-B and type V-A CRISPR-Cas systems in the opportunistic human pathogen *Francisella tularensis* subspecies *novicida* Utah 112 (here *F. novicida* U112) (Fig. S1A-B)[13,36,37]. It has been shown previously that both *F. novicida* systems are functional and capable of restricting foreign DNA[38,39]. Interestingly, *F. novicida* Cas9 is also required for virulence and enhances membrane stability by repressing an operon containing a lipoprotein with unknown function[40–43]. Using florescence microscopy, we found that the two *F. novicida* CRISPR-Cas systems are differentially regulated and expressed in non-infection conditions. While the type II-B CRISPR-Cas system is constitutively expressed, the type V-A CRISPR-Cas system displays significantly higher expression during stationary phase. Using mass spectrometry and genetics we identified MtvS (Modulator of the type V-A CRISPR-Cas system expression in stationary phase, FTN_1238), a protein with previously unknown function in *Francisella* species, as a factor required for the differential expression of the type V-A CRISPR-Cas locus. Last, we showed that type V-A CRISPR-Cas system expression is induced upon introduction to spent overnight medium suggesting that *F. novicida* is capable of quorum sensing despite lacking canonical quorum sensing genes.

Results

*The F. novicida Type V-A CRISPR-*cas *locus is upregulated during stationary phase*

55 To investigate the expression pattern of the type II-B and type V-A CRISPR-Cas systems in
56 *F. novicida* U112, their RNA-guided nucleases were C-terminally tagged to generate Cas9-
57 msfGFP and Cas12-mCherry2, respectively. The fluorescent tags did not affect their nuclease
58 function, since plasmid interference assays confirmed that the tagged nucleases prevented
59 plasmid conjugation as well as the native ones (Fig. S1C). Fluorescence live-cell imaging of
60 exponentially growing bacteria and cells in stationary phase revealed that fluorescence
61 intensity was comparable in both growth phases for Cas9-msfGFP while fluorescent intensity
62 for Cas12-mCherry2 was higher in stationary phase (Fig. 1A). We then performed RNA-seq
63 to test if the distinct expression patterns of the two effector nucleases originate from different
64 transcription levels. Comparing RNA levels of genes between exponentially growing and
65 stationary phase bacteria confirmed that *cas12* and $cas1_{typeV\text{-}A}$ RNA levels are significantly
66 higher during stationary phase than in exponential growth phase (Fig. 1B). In comparison, all
67 components from the type II-B CRISPR-Cas system, including *cas9*, had comparable RNA
68 levels in the two tested conditions (Fig. 1B). Calculated expression changes between
69 exponential and stationary growth for all genes are listed in the Supplementary Data File.
70 Targeted measurement of RNA levels of *cas9* and *cas12* by RT-qPCR confirmed the
71 invariability of RNA levels of *cas9* in the two tested growth conditions and the distinct
72 temporal expression of *cas12* in stationary growth phase (Fig. 1C and D). Together these
73 results show that the two effector nucleases from the *Francisella* type II-B and type V-A
74 CRISPR-Cas systems have different expression patterns and that *cas12* expression levels
75 significantly increase in stationary phase.

76 *MtvS is required for upregulation of the Type V-A CRISPR-cas locus in stationary phase*

77 Type V-A CRISPR-Cas systems have been shown to autoregulate in an RNA-guided and Cas
78 effector dependent manner[30]. Moreover, *F. novicida* U112 *cas12* promoter sequence contains
79 a predicted small repeat unit (SRU, with a similar but not identical sequence to the canonical
80 CRISPR repeat, Fig. 2A), which was proposed to have a regulatory function[29]. To test if
81 Cas12 is responsible for the upregulation of the type V-CRISPR-*cas* locus we replaced *cas12*
82 with *mCherry2*. However, the fluorescence pattern did not change in absence of *cas12* (Fig.
83 2B). In addition, deletion of the predicted regulatory *SRU* sequence in the *cas12* promoter
84 sequence did not result in any significant changes in *cas12* RNA levels or targeting efficiency
85 (Fig. 2C-D). To identify other transcription factors, we performed a protein pull down using
86 the *cas12* promoter DNA sequence and an intragenic *cas12* control sequence as bait. Lysates
87 from exponentially growing and stationary bacteria were probed and pull-down proteins were
88 identified proteins by LC-MS/MS. All identified proteins are listed in the Supplementary Data

File. An enrichment score was calculated by comparing protein abundance in pull downs from the *cas12* promoter sequence to the control sequence. In exponentially growing cells, one of the most significantly enriched proteins was the LysR-family transcriptional regulator FTN_0392 (Fig. 3A, Supplementary Data File). However, neither Cas12-mCherry2 expression nor targeting capability was decreased in a *FTN_0392* deletion mutant (Fig. S2A-B). On the other hand, in the stationary growth sample, FTN_1238 was significantly enriched (Fig. 3B). Importantly, there was no enrichment for FTN_1238 when using a lysate from exponentially growing bacteria (Fig. 3A). *FTN_1238* is the first gene of an operon encoding for genes required for the respiratory chain (*ubiH*, *ubiF*), a putative phage protein (*FTN_1235*) and a tRNA modification enzyme (*queA*) (Fig. S2C). FTN_1238 has no assigned function in *Francisella* yet but is homologous to YgfB (Fig. S2D), which is conserved in many γ-proteobacteria [44].

To test if FTN_1238 was involved in regulation of *cas12* expression, we made a non-sense mutation by introducing three stop codons after aspartate at position 11 and analyzed the mutant cultures via fluorescence microscopy. We found decreased fluorescence of Cas12-mCherry2 in stationary phase for this mutant (Fig. 3C) and the phenotype could be rescued by introducing a wild-type copy of *FTN_1238* with its native promoter at the Tn7 introduction site downstream of gene *glmS* (*FTN_0485*) (Fig. 3C). Disruption of FTN_1238 significantly affected the RNA levels of all type V-A CRISPR-Cas system genes in stationary phase as measured by RT-qPCR (Fig. 3D-G). RNA levels were also restored with an additional wild-type copy of *FTN_1238* (Fig. 3D-G) except for *cas2*, the last gene of the operon (Fig. 3G). Importantly, *cas9* RNA levels were not affected (Fig. S3B), a result that demonstrates that FTN_1238 acts specifically on the type V-A locus. Interestingly, while disruption of *FTN_1238* had a detrimental effect on *cas12* RNA levels in stationary phase, targeting capability of Cas12 in plasmid interference assays was not affected (Fig. S2E), most likely due to the presence of low levels of Cas12 that are sufficient to clear the invading plasmid. Finally, while *FTN_1238* RNA levels were comparable in both growth phases (Fig. S2F, Supplementary Data File), fluorescence microscopy suggested higher proteins levels of FTN_1238-mCherry2 in stationary phase (Fig. S2G). In summary, our results indicate that FTN_1238 is a <u>m</u>odulator of the <u>t</u>ype <u>V-A</u> CRISPR-Cas system expression in <u>s</u>tationary phase, and therefore we renamed it MtvS.

*Quorum sensing signals participate in the regulation of the Type V-A CRISPR-*cas *locus*

121 During stationary phase the cell density is high (Figs. 1 and 3). Interestingly, microscopy of
122 exponentially growing cells in microfluidic plates showed that Cas12-mCherry2 is also
123 expressed in a MtvS dependent manner in this growing phase within densely populated areas
124 (Fig. 4A-B, Movies 1 and 3), but not in less dense regions belonging to the same flow
125 chamber (Fig. 4A-B, Movies 2-4). These results led us to hypothesize that quorum sensing
126 could play a role in regulating the type V-A CRISPR-Cas system. Therefore, we tested if the
127 addition of spent overnight medium could increase *cas12* expression in exponential cultures
128 of *F. novicida* U112, possible containing signals that would trigger expression. We replaced
129 the medium of exponentially growing cells with filtered spent overnight medium in
130 microfluidic plates and monitored individual cells by microscopy. We observed drastic
131 changes, with bacteria changing from rod to coccus shapes, and an increased Cas12-
132 mCherry2 fluorescence (Fig. 4C, Movie 5). Fresh medium reversed these changes and cells
133 resumed growth as rod-shaped and Cas12-mCherry2 expression decreased (Fig. 4D, Movie
134 5). Heat-treatment of the spent overnight medium eliminated its activity on exponentially
135 growing bacteria (Fig. S3A, Movie 6). When exposed to overnight spent medium, *mtvS*
136 nonsense mutant cultures also suffered rod-to-coccus shape changes, but displayed much
137 lower Cas12-mCherry fluorescent signal, indicating that Cas12-mCherry2 was less expressed
138 (Fig. 4E-F, Movie 7). This result was confirmed by RT-qPCR, sampling *mtvS* nonsense
139 mutant cells before, 0.5 h and 1 h after switching to spent overnight medium and probed for
140 *cas12* and *cas9* RNA levels. While *cas12* RNA levels increased over 1 h after the medium
141 change, *cas9* RNA levels did not significantly change (Fig. 4H and Fig. S3B). Together these
142 results suggest that *F. novicida* U112 likely integrates quorum sensing signals into the MtvS
143 dependent regulation of Cas12 expression.

144

145 **Discussion**

146 Here we compared the expression of the two native type II-B and type V-A CRISPR-Cas
147 systems in *F. novicida* U112 in the absence of phage infection. We found that while the type
148 II-B CRISPR-Cas system is continuously expressed throughout growth in liquid culture, the
149 type V-A CRISPR-Cas system is significantly upregulated at high cell density and stationary
150 growth phase. We envision different possibilities behind this unique regulation. First, it is
151 known that bacteria enhance their anti-phage defenses in high cell density environments when
152 they are more vulnerable to phage predation[15,16,45–51]. Given that the type II-B system is
153 constitutively expressed, the upregulation of the type V-A system will equip *F. novicida* U112

154 with additional defenses in stationary phase. Moreover, our RNA-seq analysis also found
155 upregulation of two of the six annotated restriction-modification systems in stationary growth
156 phase (Supplementary Data File 1)[52]. It is also possible that Cas12 or other components of the
157 type V-A CRISPR-Cas system have a role beyond immunity in stationary growth phase,
158 analogous to the function of *F. novicida* Cas9 in the regulation of lipoprotein expression[40–43].
159 Our RNA-seq experiment showed drastic changes in transcription in stationary phase,
160 indicating the need to adapt to this growth condition, an adaptation in which Cas12 could play
161 a part that would justify its upregulation in this growth phase.

162 We identified MtvS (FTN_1238), a protein with previously unknown function in *F. novicida*
163 U112, as a factor required for the upregulation of the type V-A CRISPR-Cas system in
164 stationary phase and upon addition of spent overnight medium to the exponentially growing
165 cultures. MtvS belongs to the YecA/YgfB-like protein family and is conserved in many γ-
166 proteobacteria[44]. Besides the structure of *Haemophilus influenzae* YgfB, little is known about
167 the function of this family of proteins[53]. In *Pseudomonas aeruginosa*, YgfB increases β-
168 lactam resistance [54] through interactions with the antitermination factor AlpA that lead to the
169 upregulation of AmpC expression[55]. We believe that it is unlikely that MtvS interacts with an
170 antitermination factor to upregulate the type V-A CRISPR locus in *F. novicida* U112 since
171 *cas12* transcription decreases in the *mtvS* mutant (Fig. 3). We were unable to detect specific
172 binding to the *cas12* promoter region by purified MtvS (data not shown), therefore we
173 hypothesize that MtvS either stimulates *cas12* transcription through interaction with other
174 factors or with RNA polymerase or through the inhibition of a termination factor.
175 Intriguingly, mass spectrometry analysis of pull-downs showed enrichment for NusA, which
176 can act both as transcriptional termination and antitermination factor depending on the
177 bacterial species, as well as transcriptional termination factor Rho (Supplementary Data File
178 1). Unfortunately, due to the essential nature of NusA and Rho in *F. novicida* U112[56], we
179 were unable to create knock out strains to investigate a possible role for these factors in the
180 modulation of the type V-A CRISPR locus. Finally, *mtvS* RNA levels were comparable in
181 both growth conditions but MtvS-mCherry2 levels increased in stationary phase. Therefore, it
182 is likely that MtvS is post-transcriptionally regulated.

183 *F. novicida* U112 cells reacted strongly to spent overnight medium, displaying a growth
184 arrest, morphology changes and an increase in Cas12 expression, the latter also dependent on
185 the presence of MtvS. Changes in gene expression as reaction to spent overnight medium is a
186 hallmark of quorum sensing[57]. However, *F. novicida* U112 lacks canonical quorum sensing

187 genes[58]. Our results suggest that the type V-A CRISPR-Cas system and MtvS could be part of
188 a quorum sensing circuit that monitors and responds to changes in cell density. Future studies
189 will investigate this possibility, relevant not only for the understanding of the phage defense
190 strategies but also for the pathogenesis of *Francisella*.

Author Contributions. M.B. and L.A.M. conceived the study. M.B. performed all experiments. M.B. and L.A.M. wrote the manuscript. All authors read and approved the manuscript.

Acknowledgments. We thank D.M. Monack (Stanford University) for the conjugation plasmid pDMK3, A. Harms (ETH Zurich) and C. Dehio (Biozentrum, University of Basel) for the *E. coli* conjugation strain, M. Basler (Biozentrum, University of Basel) for plasmid pFNMB2 *msfGFP*, E. Campbell (The Rockefeller University) for helpful scientific discussions and H. Molina and C. Peralta (Proteomics Resource Center, The Rockefeller University) for performing and analyzing the LC-MS/MS experiment. Proteomics data was generated by the Proteomics Resource Center at The Rockefeller University (RRID:SCR_017797) using instrumentation funded by the Sohn Conferences Foundation and the Leona M. and Harry B. Helmsley Charitable Trust. Thanks also goes to C.F. Baca (The Rockefeller University) for scientific advice and support and to all members of the Marraffini lab (The Rockefeller University) for scientific discussions and feedback. M.B. was supported by the SNSF Early Postdoc.Mobility (P2BSP3_195673) and SNSF Postdoc.Mobility (P500PB_210998) fellowships. L.A.M. is an investigator of the Howard Hughes Medical Institute.

Competing interests. LAM is a cofounder and Scientific Advisory Board member of Intellia Therapeutics, a cofounder of Eligo Biosciences and a Scientific Advisory Board member of Ancilia Biosciences.

211 **Material and Methods**

212 **Bacterial strains and growth conditions**

213 *Francisella novicida* U112 (*F. novicida* U112) and associated mutants were grown
214 aerobically in brain heart infection (BHI, BD Biosciences) broth or on BHI agar plates
215 supplemented with 0.1 % L-cysteine (Sigma Alderich) and 50 µg/ml ampicillin (GoldBio). F.
216 *novicida* strains carrying plasmids were grown with 15 µg/ml kanamycin (GoldBio).

217 To receive exponentially growing cultures, stationary phase cells were diluted 1:20 in fresh
218 media and grown for 2-3 h until they reached an OD_{600} of 0.5-0.8 and had a rod-shaped
219 morphology. Stationary phase cells were grown over night for at least 16 hours until they
220 reached an OD_{600} of 3.5-4.5 and displayed a more coccus-like cell shape. Cell morphology
221 was checked by microscopy.

222 *Escherichia coli* OneShotpir (*E. coli,* ThermoFisher) and derivative strains were aerobically
223 grown in Luria broth (LB, BD Biosciences) or on LB agar plates supplemented with 50 µg/ml
224 kanamycin at 37 °C. For conjugation *E. coli* JKE201 1.2 mM 2,6-Diaminopimelic acid (DAP,
225 Sigma Alderich) was added to all growth media since this strain is auxotrophic for mDAP.
226 Strains used for this study are listed in table 1.

227

228 **Bacterial mutagenesis**

229 To generate chromosomal in-frame *F. novicida* mutants, suicide vector pDMK3 was used [59].
230 For fluorescent tags, an Ala-Ala-Ala-Gly-Gly-Gly linker was added and after the stop codon
231 the 30 bp sequence of the gene was repeated to avoid downstream polar affects. For the His-
232 tags only a Gly linker was added. In-frame deletions yielded in peptide scars containing the
233 first and last 10 amino acids. Mutagenesis and conjugation was carried out as reported
234 previously [60,61]. For conjugation, donor *E. coli* JKE201 from A. Harms and C. Dehio [62] and
235 recipient *F. novicida* strains were grown until a OD_{600} of 1 was reached. 1 ml of each culture
236 was mixed in 20 µl of LB and spotted on a LB agar plate supplemented with 1.2 mM DAP
237 and incubated over night at 25 °C. The mixture was plated on Mueller Hinton (BD
238 Biosciences) agar plates supplemented with 0.1 % L-cysteine, 0.1 % D-glucose (Sigma
239 Alderich), 0.1 % heat inactivated fetal calf serum (Gibco), 50 µg/ml ampicillin and 15 µg/ml
240 kanamycin and incubated at 37 °C for 2 days. *F. novicida* colonies containing the suicide
241 vector were restreaked on BHI agar plates supplemented with 15 µg/ml kanamycin. To select
242 against pDMK3, individual colonies were restreaked on LB agar plates supplemented with 5
243 % sucrose (Sigma Alderich), 0.1 % L-cysteine and 50 µg/ml ampicillin and incubated at 25
244 °C until colonies lost the suicide vector. Each mutant was verified by colony PCR using
245 primers binding outside of the recombined region and sequencing of these regions. In
246 addition, they were restreaked on kanamycin again to check for loss of pDMK3.

247 All primers and plasmids are listed in table 2.

248

249 **Fluorescence live cell imaging**

250 A Nikon Ti-E inverted motorized microscope equipped with Perfect Focus System and a CFI
251 Plan Apochromat DM Lambda 100X Oil objective lens (NA 1.4) was used for live-cell
252 imaging. A SOLA Light Engine (Lumencor) set to 5 % power and C-FL GFP HC HISN Zero
253 Shift filter (excitation: 470/40 nm (450–490 nm), emission: 525/50 nm (500–550 nm),
254 dichroic mirror: 495 nm) and C-FL DS RED HC HISN Zero Shift filters (excitation:
255 545/30nm (530-560nm), emission: 620/60nm (590-630nm), dichroic mirror: 570nm),
256 respectively, were used to excite and filter fluorescence from msfGFP and mCherry2. The

exposure time for each channel was set to 500 ms and images were collected with a Zyla 4.2 sCMOS (Andor, pixel size 65 nm) or an ORCA-FusionBT sCMOS camera (Hamamatsu, pixel size 65 nm). Phase contrast was imaged with the SOLA light Engine set to 2% power and 10 ms excitation. The microscope was controlled by the software NIS-Elements AR version 5.21.03.

Exponentially grown (rod-shaped) and stationary phase (roundish) *F. novicida* were spun down and resuspended in phosphate saline buffer (PBS, Gibco) and spotted on pads consisting of 1% agarose in PBS. Snapshots of phase contrast, RFP and GFP channels were taken immediately after.

Long-term imaging experiments which include switching of media were carried out in CellASIC ONIX microfluidic plates (Millipore). Exponentially growing bacteria were resuspended in BHI supplemented with 0.2 % L-cysteine and loaded into the microfluidic plate along with fresh BHI supplemented with 0.2 % L-cysteine for initial growth and the tested medium as specified in the Fig. legend. For generating spent overnight medium, cells in stationary phase were pelleted for 1.5 min at 16000 g and supernatant was filtered with 0.22 µm filters (Millipore). For heat-treated spent overnight medium, filtered spent overnight medium was incubated at 95 °C for 10-20 min. After connecting the plate to the CellASIC ONIX2 Microfluidic System, the plates were incubated at 37 °C for 1 h using a Tokai HIT thermal box (Zeiss). Images of phase contrast, RFP and GFP channel were taken every 5 minutes after loading cells into the imaging chamber. First, fresh BHI was flown over for 1 h before switching to the tested medium for 4h. Afterwards, fresh BHI was flown over again for 3 h. For all media, the flow rate was set to 13.8 kPa.

Image analysis

Image analysis was carried out with Fiji software [63]. For comparison of fluorescent signal intensities, the contrast was set to same values for sets of compared images in same sub panel. If compared across sub panels, it is stated in Fig. legend which contrasts are set to same values.

For long-term imaging, images were aligned to the first image using NIS-Elements AR version 5.21.03.

RNA-seq

RNA was extracted from exponentially growing and stationary phase cells in three biological replicates for each condition. Cells yielding in a total OD_{600} of 3 were pelleted and resuspended in 80 µl of PBS and 20 µl of 10 % Sarcosyl (Sigma Alderich). Then, RNA was extracted with TRI Reagent according to the manufacturer's protocol (Zymo Research). An in-column DNA digest during RNA extraction was performed. A second DNA digestion was carried out with 10 µg of RNA using Turbo DNase (Invitrogen) for 2x 30 min. The DNA-free RNA was cleaned up with the RNA Clean & Concentrator-5 kit (Zymo Research) and eluted in 15 µl of water. RNA quality was checked by running a bleach agarose gel[64]. RNA concentrations were measured with a Qubit 4 fluorometer (Invitrogen) using the Qubit RNA Broad Range Assay Kit.

Ribosomal RNA was depleted with the NEBNext rRNA depletion (bacteria) kit (NEB). An input of 1 µg of RNA was used. Then, the RNA was prepared for sequencing using the TruSeq Stranded mRNA kit (Illumina) according to manufacturer's instruction. For the first strand synthesis, Superscript IV reverse transcriptase (Invitrogen) was used with an annealing temperature of 50 °C. Final DNA concentrations and lengths were measured with a Qubit 4

304 fluorometer (Invitrogen) using the Qubit dsDNA High Sensitivity Assay Kit and the
305 Tapestation 4200 bioanalyzer (Agilent) with the Agilent D500 ScreenTape Assay (Agilent).

306 The DNA libraries were diluted to 12 pM and mixed with 2.5% 20 pM PhiX and subjected to
307 single read sequencing with a 150-cycle MiSeq Reagent Kit v3 (Illumina) on the Illumina
308 MiSeq platform.

309 The reads were mapped to the *F. novicida* U112 genome (RefSeq NC_008601[65]) and RPKM
310 values for each gene was calculated using coordinates of coding genes (ptt files) and of
311 rRNAs and tRNAs (rtt files) with EDGE-Pro v1.3.1[66]. EDGE-Pro statistics for each sample
312 can be found in table 5. Significant changes in gene expression between used conditions were
313 calculated with the R (version 4.3.0) package DESeq2 (version 1.40.2)[67]. Results can be
314 found in table 6. *P*-values of 0.01 and log2 foldchanges of 2 were defined significant.

315

316 **RT-qPCR**

317 RNA was extracted as reported for RNA-seq. The RNA was reverse transcribed to cDNA
318 with Superscript IV reverse transcriptase (Invitrogen) using 1 µg of RNA, random hexamer
319 primers, and a reaction temperature of 50 °C.

320 qPCR was performed in the QuantStudio 3 Real-Time PCR System (Applied Biosystems)
321 using the PowerUp SYBR Green Master Mix (Applied Biosystems). Reactions were set up in
322 a total volume of 20 µl containing 50 ng of cDNA template and 500 nM primers. Each
323 reaction was set up in three technical replicates. All primers used for RT-qPCR are found in
324 table 3. The annealing and amplification temperature was set to 60 °C.

325 The geometrical mean of the three technical replicates for each biological replicate was used
326 for further analysis. RNA levels of probed genes were normalized to the DNA 3'-5' helicase
327 gene *uvrD* (FTN_1594), which has been used previously for normalization and does not
328 change its expression in the used conditions as determined by RNA-seq[68]. The average value
329 of the three biological *uvrD* replicates was used to the ΔCt value for each gene. Relative RNA
330 abundance of probed genes was calculated as $2^{-\Delta Ct}$.

331 Statistical analysis for RT-qPCR data was performed with Prism10.2.3 (403) (GraphPad
332 Software). To test if relative RNA abundances determined by RT-qPCR are significantly
333 different, two-way ANOVA (α=0.05) with correction for multiple comparison (Tukey's
334 multiple comparisons test) was performed. Adjusted *P*-values are given in the Fig. legends.

335

336 **Plasmid interference assay**

337 Strains were generated with the native Type II-B or Type V-A CRISPR array replaced by a
338 targeting or non-targeting spacer matching expression plasmid pFNMB2 *msfGFP*. These
339 strains were grown exponentially together with the donor *E. coli* strain harboring pFNMB2
340 *msfGFP*. Cells yielding a total OD_{600} of 1 were pelleted and washed once with LB. Then,
341 recipient *F. novicida* strains were mixed with donor *E. coli* in a final volume of 20 µl LB and
342 spotted on nitrocellulose filter membranes with a 0.22 µm pore size (Millipore) located on LB
343 agar plates supplemented with 1.2 mM DAP. The plates were incubated for 2 h at 37 °C
344 before the bacteria were resuspended in a final volume of 100 µl MH broth (BD Biosciences).
345 Serial dilutions in MH broth were carried out and 5 µl of each dilution was spotted in
346 technical duplicates on MH agar plates supplemented with 50 µg/ml ampicillin for calculation
347 of total number of colony forming units (CFUs) and on MH agar plates supplemented with 50
348 µg/ml ampicillin and 15 µg/ml kanamycin for calculation of transformants. The average

349 number of CFUs of the two technical replicates was used for calculating CFU/ml. Three
350 biological replicates for each strain were analyzed.

351

352 **Promoter sequence pull-down**

353 Pull-down of proteins binding the *cas12* promoter and the intragenic *cas12* control sequence
354 was carried out as reported previously[69,70].

355 In short, primers with a 5' Biotin-TEG label were used to generate the bait DNA sequences
356 (table 4) from *F. novicida* gDNA. PCR products were checked by agarose gel and cleaned up
357 with QIAquick PCR Purification Kit (QIAGEN) and concentrated with Amicon Ultra-0.5 mL
358 Centrifugal Filters (Millipore Sigma) to 200 ng/µl in water. Washed Dynabeads MyOne
359 Streptavidin C1 (Thermo Fisher Scientific) were loaded with 40 µg of DNA for 20 minutes.
360 DNA concentrations in the removed supernatants were measured to ensure that most DNA
361 bound to the Dynabeads. Exponentially growing and stationary phase cells yielding a total
362 OD_{600} of 800 were resuspended in 5 ml 1x FastBreak cell lysis buffer (Promega) for 30
363 minutes on ice and then sonicated afterwards. 200 µl of precleared lysates was added to the
364 resuspended beads supplemented with 0.03 µg/µl salmon sperm DNA (Thermo Fisher
365 Scientific) and incubated for 1 h with agitation. The beads were washed 2x with a wash buffer
366 (100 mM NaCl (Sigma Alderich), 25 mM Tris-HCl (VWR, Thermo Scientific), pH 7.5) and
367 then switched to new tubes before a last wash. The dried beads were stored at 4 °C until they
368 were subjected to LC-MS/MS analysis.

369

370 **LC-MS/MS analysis**

371 Beads were resuspended in 8 M Urea and proteins were recovered from beads. After
372 alkylation, proteins were digested with trypsin and LysC. The reaction was stopped with
373 trifluoroacetic acid. Generated peptides were desalted and concentrated with solid-phase
374 extraction prior to analysis by LC-MS/MS (12cm packed-in-emitter column, 70min gradient,
375 QE-HF). The raw data was searched and quantified using ProteomeDiscoverer/Mascot and
376 MaxQuant (version 2.0.3.0) using Uniprot database for *F. tularensis* subspecies *novicida*
377 U112 (taxon ID: 401614) with additional common contaminants generating the LFQ and
378 iBAQ values. Statistical analysis was carried out with Perseus software. Contaminants and
379 proteins that have been identified in less than two biological replicates of a sample were
380 removed. iBAQ were median normalized. The Log2 foldchange was calculated between
381 proteins pulled-down with the *cas12* promoter sequence and proteins pulled-down with the
382 intragenic *cas12* control sequence for both exponential and stationary conditions. An FDR-
383 based (FDR = 0.05) two sample t-test was used to determine which changes were significant.
384 *P*-values of 0.01 and log2 foldchanges of 4 were defined significant.

385

386 **Homology prediction with Foldseek**

387 Foldseek[71] was used to find structural homologs for the predicted structure of FTN_1238
388 (Uniprot ID: A0A6I4RTR9).

389

390 **Data availability**

391 Source data are provided in this paper.

392 **References**

393 1. Marraffini, L.A., and Sontheimer, E.J. (2008). CRISPR interference limits horizontal
394 gene transfer in staphylococci by targeting DNA. Science *322*, 1843–1845.
395 https://doi.org/10.1126/science.1165771.

396 2. Barrangou, R., Fremaux, C., Deveau, H., Richards, M., Boyaval, P., Moineau, S.,
397 Romero, D.A., and Horvath, P. (2007). CRISPR provides acquired resistance against viruses in
398 prokaryotes. Science *315*, 1709–1712. https://doi.org/10.1126/science.1138140.

399 3. Bolotin, A., Quinquis, B., Sorokin, A., and Ehrlich, S.D. 2005 Clustered regularly
400 interspaced short palindrome repeats (CRISPRs) have spacers of extrachromosomal origin.
401 Microbiology *151*, 2551–2561. https://doi.org/10.1099/mic.0.28048-0.

402 4. Mojica, F.J.M., Díez-Villaseñor, C., García-Martínez, J., and Soria, E. (2005).
403 Intervening Sequences of Regularly Spaced Prokaryotic Repeats Derive from Foreign Genetic
404 Elements. J. Mol. Evol. *60*, 174–182. https://doi.org/10.1007/s00239-004-0046-3.

405 5. Pourcel, C., Salvignol, G., and Vergnaud, G.Y. 2005 CRISPR elements in Yersinia
406 pestis acquire new repeats by preferential uptake of bacteriophage DNA, and provide additional
407 tools for evolutionary studies. Microbiology *151*, 653–663.
408 https://doi.org/10.1099/mic.0.27437-0.

409 6. Brouns, S.J.J., Jore, M.M., Lundgren, M., Westra, E.R., Slijkhuis, R.J.H., Snijders,
410 A.P.L., Dickman, M.J., Makarova, K.S., Koonin, E.V., and Oost, J. van der (2008). Small
411 CRISPR RNAs Guide Antiviral Defense in Prokaryotes. Science.
412 https://doi.org/10.1126/science.1159689.

413 7. Hale, C., Kleppe, K., Terns, R.M., and Terns, M.P. (2008). Prokaryotic silencing
414 (psi)RNAs in Pyrococcus furiosus. RNA N. Y. N *14*, 2572–2579.
415 https://doi.org/10.1261/rna.1246808.

416 8. Abudayyeh, O.O., Gootenberg, J.S., Konermann, S., Joung, J., Slaymaker, I.M., Cox,
417 D.B.T., Shmakov, S., Makarova, K.S., Semenova, E., Minakhin, L., et al. (2016). C2c2 is a
418 single-component programmable RNA-guided RNA-targeting CRISPR effector. Science *353*,
419 aaf5573. https://doi.org/10.1126/science.aaf5573.

420 9. Gasiunas, G., Barrangou, R., Horvath, P., and Siksnys, V. (2012). Cas9-crRNA
421 ribonucleoprotein complex mediates specific DNA cleavage for adaptive immunity in bacteria.
422 Proc. Natl. Acad. Sci. U. S. A. *109*, E2579-2586. https://doi.org/10.1073/pnas.1208507109.

423 10. Hale, C.R., Zhao, P., Olson, S., Duff, M.O., Graveley, B.R., Wells, L., Terns, R.M., and
424 Terns, M.P. (2009). RNA-Guided RNA Cleavage by a CRISPR RNA-Cas Protein Complex.
425 Cell *139*, 945–956. https://doi.org/10.1016/j.cell.2009.07.040.

426 11. Jinek, M., Chylinski, K., Fonfara, I., Hauer, M., Doudna, J.A., and Charpentier, E.
427 (2012). A programmable dual-RNA-guided DNA endonuclease in adaptive bacterial immunity.
428 Science *337*, 816–821. https://doi.org/10.1126/science.1225829.

429 12. Westra, E.R., van Erp, P.B.G., Künne, T., Wong, S.P., Staals, R.H.J., Seegers, C.L.C.,
430 Bollen, S., Jore, M.M., Semenova, E., Severinov, K., et al. (2012). CRISPR immunity relies on
431 the consecutive binding and degradation of negatively supercoiled invader DNA by Cascade
432 and Cas3. Mol. Cell *46*, 595–605. https://doi.org/10.1016/j.molcel.2012.03.018.

13. Zetsche, B., Gootenberg, J.S., Abudayyeh, O.O., Slaymaker, I.M., Makarova, K.S., Essletzbichler, P., Volz, S.E., Joung, J., van der Oost, J., Regev, A., et al. (2015). Cpf1 is a single RNA-guided endonuclease of a class 2 CRISPR-Cas system. Cell *163*, 759–771. https://doi.org/10.1016/j.cell.2015.09.038.

14. Makarova, K.S., Wolf, Y.I., Iranzo, J., Shmakov, S.A., Alkhnbashi, O.S., Brouns, S.J.J., Charpentier, E., Cheng, D., Haft, D.H., Horvath, P., et al. (2020). Evolutionary classification of CRISPR-Cas systems: a burst of class 2 and derived variants. Nat. Rev. Microbiol. *18*, 67–83. https://doi.org/10.1038/s41579-019-0299-x.

15. Patterson, A.G., Jackson, S.A., Taylor, C., Evans, G.B., Salmond, G.P.C., Przybilski, R., Staals, R.H.J., and Fineran, P.C. (2016). Quorum Sensing Controls Adaptive Immunity through the Regulation of Multiple CRISPR-Cas Systems. Mol. Cell *64*, 1102–1108. https://doi.org/10.1016/j.molcel.2016.11.012.

16. Høyland-Kroghsbo, N.M., Paczkowski, J., Mukherjee, S., Broniewski, J., Westra, E., Bondy-Denomy, J., and Bassler, B.L. (2017). Quorum sensing controls the Pseudomonas aeruginosa CRISPR-Cas adaptive immune system. Proc. Natl. Acad. Sci. U. S. A. *114*, 131–135. https://doi.org/10.1073/pnas.1617415113.

17. Lucas-Elío, P., Molina-Quintero, L.R., Xu, H., and Sánchez-Amat, A. (2021). A histidine kinase and a response regulator provide phage resistance to Marinomonas mediterranea via CRISPR-Cas regulation. Sci. Rep. *11*, 20564. https://doi.org/10.1038/s41598-021-99740-9.

18. Borges, A.L., Castro, B., Govindarajan, S., Solvik, T., Escalante, V., and Bondy-Denomy, J. (2020). Bacterial alginate regulators and phage homologs repress CRISPR-Cas immunity. Nat. Microbiol. *5*, 679–687. https://doi.org/10.1038/s41564-020-0691-3.

19. Perez-Rodriguez, R., Haitjema, C., Huang, Q., Nam, K.H., Bernardis, S., Ke, A., and DeLisa, M.P. (2011). Envelope stress is a trigger of CRISPR RNA-mediated DNA silencing in Escherichia coli. Mol. Microbiol. *79*, 584–599. https://doi.org/10.1111/j.1365-2958.2010.07482.x.

20. Pul, U., Wurm, R., Arslan, Z., Geissen, R., Hofmann, N., and Wagner, R. (2010). Identification and characterization of E. coli CRISPR-cas promoters and their silencing by H-NS. Mol. Microbiol. *75*, 1495–1512. https://doi.org/10.1111/j.1365-2958.2010.07073.x.

21. Westra, E.R., Pul, U., Heidrich, N., Jore, M.M., Lundgren, M., Stratmann, T., Wurm, R., Raine, A., Mescher, M., Van Heereveld, L., et al. (2010). H-NS-mediated repression of CRISPR-based immunity in Escherichia coli K12 can be relieved by the transcription activator LeuO. Mol. Microbiol. *77*, 1380–1393. https://doi.org/10.1111/j.1365-2958.2010.07315.x.

22. Kang, D.-Y., Kim, A., and Kim, J.N. (2023). CcpA and CodY Regulate CRISPR-Cas System of Streptococcus mutans. Microbiol. Spectr., e0182623. https://doi.org/10.1128/spectrum.01826-23.

23. Smith, L.M., Hampton, H.G., Yevstigneyeva, M.S., Mahler, M., Paquet, Z.S.M., and Fineran, P.C. (2023). CRISPR-Cas immunity is repressed by the LysR-type transcriptional regulator PigU. Nucleic Acids Res., gkad1165. https://doi.org/10.1093/nar/gkad1165.

24. Zhang, Y., Yang, J., and Bai, G. (2018). Regulation of the CRISPR-Associated Genes by Rv2837c (CnpB) via an Orn-Like Activity in Tuberculosis Complex Mycobacteria. J. Bacteriol. *200*, e00743-17. https://doi.org/10.1128/JB.00743-17.

25. Patterson, A.G., Chang, J.T., Taylor, C., and Fineran, P.C. (2015). Regulation of the Type I-F CRISPR-Cas system by CRP-cAMP and GalM controls spacer acquisition and interference. Nucleic Acids Res. *43*, 6038–6048. https://doi.org/10.1093/nar/gkv517.

26. Smith, L.M., Jackson, S.A., Malone, L.M., Ussher, J.E., Gardner, P.P., and Fineran, P.C. (2021). The Rcs stress response inversely controls surface and CRISPR-Cas adaptive immunity to discriminate plasmids and phages. Nat. Microbiol. *6*, 162–172. https://doi.org/10.1038/s41564-020-00822-7.

27. Medina-Aparicio, L., Rebollar-Flores, J.E., Gallego-Hernández, A.L., Vázquez, A., Olvera, L., Gutiérrez-Ríos, R.M., Calva, E., and Hernández-Lucas, I. (2011). The CRISPR/Cas immune system is an operon regulated by LeuO, H-NS, and leucine-responsive regulatory protein in Salmonella enterica serovar Typhi. J. Bacteriol. *193*, 2396–2407. https://doi.org/10.1128/JB.01480-10.

28. He, F., Vestergaard, G., Peng, W., She, Q., and Peng, X. (2017). CRISPR-Cas type I-A Cascade complex couples viral infection surveillance to host transcriptional regulation in the dependence of Csa3b. Nucleic Acids Res. *45*, 1902–1913. https://doi.org/10.1093/nar/gkw1265.

29. Shmakov, S.A., Barth, Z.K., Makarova, K.S., Wolf, Y.I., Brover, V., Peters, J.E., and Koonin, E.V. (2023). Widespread CRISPR repeat-like RNA regulatory elements in CRISPR-Cas systems. Preprint at bioRxiv, https://doi.org/10.1101/2023.03.03.530964 https://doi.org/10.1101/2023.03.03.530964.

30. Liu, C., Wang, R., Li, J., Cheng, F., Shu, X., Zhao, H., Xue, Q., Yu, H., Wu, A., Wang, L., et al. (2023). Widespread RNA-based cas regulation monitors crRNA abundance and anti-CRISPR proteins. Cell Host Microbe *31*, 1481-1493.e6. https://doi.org/10.1016/j.chom.2023.08.005.

31. Workman, R.E., Pammi, T., Nguyen, B.T.K., Graeff, L.W., Smith, E., Sebald, S.M., Stoltzfus, M.J., Euler, C.W., and Modell, J.W. (2021). A natural single-guide RNA repurposes Cas9 to autoregulate CRISPR-Cas expression. Cell *184*, 675-688.e19. https://doi.org/10.1016/j.cell.2020.12.017.

32. Liu, T., Li, Y., Wang, X., Ye, Q., Li, H., Liang, Y., She, Q., and Peng, N. (2015). Transcriptional regulator-mediated activation of adaptation genes triggers CRISPR de novo spacer acquisition. Nucleic Acids Res. *43*, 1044–1055. https://doi.org/10.1093/nar/gku1383.

33. Maharajan, A.D., Hjerde, E., Hansen, H., and Willassen, N.P. (2022). Quorum Sensing Controls the CRISPR and Type VI Secretion Systems in Aliivibrio wodanis 06/09/139. Front. Vet. Sci. *9*, 799414. https://doi.org/10.3389/fvets.2022.799414.

34. Bilger, R., Migur, A., Wulf, A., Steglich, C., Urlaub, H., and Hess, W.R. (2024). A type III-Dv CRISPR-Cas system is controlled by the transcription factor RpaB and interacts with the DEAD-box RNA helicase CrhR. Cell Rep. *43*, 114485. https://doi.org/10.1016/j.celrep.2024.114485.

514 35. Kim, H., and Marraffini, L.A. (2024). Cas9 interaction with the tracrRNA nexus
515 modulates the repression of type II-A CRISPR-cas genes. Nucleic Acids Res., gkae597.
516 https://doi.org/10.1093/nar/gkae597.

517 36. Schunder, E., Rydzewski, K., Grunow, R., and Heuner, K. (2013). First indication for a
518 functional CRISPR/Cas system in Francisella tularensis. Int. J. Med. Microbiol. IJMM *303*, 51–
519 60. https://doi.org/10.1016/j.ijmm.2012.11.004.

520 37. Fonfara, I., Richter, H., Bratovič, M., Le Rhun, A., and Charpentier, E. (2016). The
521 CRISPR-associated DNA-cleaving enzyme Cpf1 also processes precursor CRISPR RNA.
522 Nature *532*, 517–521. https://doi.org/10.1038/nature17945.

523 38. Ratner, H.K., and Weiss, D.S. (2020). F. novicida CRISPR-Cas systems can
524 functionally complement each other in DNA defense while providing target flexibility. J.
525 Bacteriol. https://doi.org/10.1128/JB.00670-19.

526 39. Ratner, H.K., and Weiss, D.S. (2021). crRNA complementarity shifts endogenous
527 CRISPR-Cas systems between transcriptional repression and DNA defense. RNA Biol., 1–14.
528 https://doi.org/10.1080/15476286.2021.1878335.

529 40. Sampson, T.R., Saroj, S.D., Llewellyn, A.C., Tzeng, Y.-L., and Weiss, D.S. (2013). A
530 CRISPR/Cas system mediates bacterial innate immune evasion and virulence. Nature *497*, 254–
531 257. https://doi.org/10.1038/nature12048.

532 41. Sampson, T.R., Saroj, S.D., Llewellyn, A.C., Tzeng, Y.-L., and Weiss, D.S. (2019).
533 Author Correction: A CRISPR/Cas system mediates bacterial innate immune evasion and
534 virulence. Nature *570*, E30–E31. https://doi.org/10.1038/s41586-019-1253-9.

535 42. Sampson, T.R., Napier, B.A., Schroeder, M.R., Louwen, R., Zhao, J., Chin, C.-Y.,
536 Ratner, H.K., Llewellyn, A.C., Jones, C.L., Laroui, H., et al. (2014). A CRISPR-Cas system
537 enhances envelope integrity mediating antibiotic resistance and inflammasome evasion. Proc.
538 Natl. Acad. Sci. U. S. A. *111*, 11163–11168. https://doi.org/10.1073/pnas.1323025111.

539 43. Ratner, H.K., Escalera-Maurer, A., Le Rhun, A., Jaggavarapu, S., Wozniak, J.E.,
540 Crispell, E.K., Charpentier, E., and Weiss, D.S. (2019). Catalytically Active Cas9 Mediates
541 Transcriptional Interference to Facilitate Bacterial Virulence. Mol. Cell *75*, 498-510.e5.
542 https://doi.org/10.1016/j.molcel.2019.05.029.

543 44. Bell, R.T., Wolf, Y.I., and Koonin, E.V. (2020). Modified base-binding EVE and DCD
544 domains: striking diversity of genomic contexts in prokaryotes and predicted involvement in a
545 variety of cellular processes. BMC Biol. *18*, 159. https://doi.org/10.1186/s12915-020-00885-2.

546 45. Tan, D., Svenningsen, S.L., and Middelboe, M. (2015). Quorum Sensing Determines
547 the Choice of Antiphage Defense Strategy in Vibrio anguillarum. mBio *6*, e00627.
548 https://doi.org/10.1128/mBio.00627-15.

549 46. Gao, R., Krysciak, D., Petersen, K., Utpatel, C., Knapp, A., Schmeisser, C., Daniel, R.,
550 Voget, S., Jaeger, K.-E., and Streit, W.R. (2015). Genome-wide RNA sequencing analysis of
551 quorum sensing-controlled regulons in the plant-associated Burkholderia glumae PG1 strain.
552 Appl. Environ. Microbiol. *81*, 7993–8007. https://doi.org/10.1128/AEM.01043-15.

553 47. Dela Ahator, S., Liu, Y., Wang, J., and Zhang, L.-H. (2022). The virulence factor
554 regulator and quorum sensing regulate the type I-F CRISPR-Cas mediated horizontal gene

555 transfer in Pseudomonas aeruginosa. Front. Microbiol. *13*, 987656.
556 https://doi.org/10.3389/fmicb.2022.987656.

557 48. Nuñez, J.K., Bai, L., Harrington, L.B., Hinder, T.L., and Doudna, J.A. (2016). CRISPR
558 Immunological Memory Requires a Host Factor for Specificity. Mol. Cell *62*, 824–833.
559 https://doi.org/10.1016/j.molcel.2016.04.027.

560 49. Ali Azam, T., Iwata, A., Nishimura, A., Ueda, S., and Ishihama, A. (1999). Growth
561 phase-dependent variation in protein composition of the Escherichia coli nucleoid. J. Bacteriol.
562 *181*, 6361–6370. https://doi.org/10.1128/JB.181.20.6361-6370.1999.

563 50. Kretz, J., Börner, J., Friedrich, T., McIntosh, M., Procida-Kowalski, T., Gerken, F.,
564 Wilhelm, J., and Klug, G. (2024). Function of the RNA-targeting class 2 type VI CRISPR Cas
565 system of Rhodobacter capsulatus. Front. Microbiol. *15*, 1384543.
566 https://doi.org/10.3389/fmicb.2024.1384543.

567 51. Høyland-Kroghsbo, N.M., Maerkedahl, R.B., and Svenningsen, S.L. (2013). A quorum-
568 sensing-induced bacteriophage defense mechanism. mBio *4*, e00362-00312.
569 https://doi.org/10.1128/mBio.00362-12.

570 52. Gallagher, L.A., McKevitt, M., Ramage, E.R., and Manoil, C. (2008). Genetic
571 dissection of the Francisella novicida restriction barrier. J. Bacteriol. *190*, 7830–7837.
572 https://doi.org/10.1128/JB.01188-08.

573 53. Galkin, A., Sarikaya, E., Lehmann, C., Howard, A., and Herzberg, O. (2004). X-ray
574 structure of HI0817 from Haemophilus influenzae: protein of unknown function with a novel
575 fold. Proteins *57*, 874–877. https://doi.org/10.1002/prot.20260.

576 54. Sonnabend, M.S., Klein, K., Beier, S., Angelov, A., Kluj, R., Mayer, C., Groß, C.,
577 Hofmeister, K., Beuttner, A., Willmann, M., et al. (2020). Identification of Drug Resistance
578 Determinants in a Clinical Isolate of Pseudomonas aeruginosa by High-Density Transposon
579 Mutagenesis. Antimicrob. Agents Chemother. *64*, e01771-19.
580 https://doi.org/10.1128/AAC.01771-19.

581 55. Eggers, O., Renschler, F.A., Michalek, L.A., Wackler, N., Walter, E., Smollich, F.,
582 Klein, K., Sonnabend, M.S., Egle, V., Angelov, A., et al. (2023). YgfB increases β-lactam
583 resistance in Pseudomonas aeruginosa by counteracting AlpA-mediated ampDh3 expression.
584 Commun. Biol. *6*, 254. https://doi.org/10.1038/s42003-023-04609-4.

585 56. Gallagher, L.A., Ramage, E., Jacobs, M.A., Kaul, R., Brittnacher, M., and Manoil, C.
586 (2007). A comprehensive transposon mutant library of Francisella novicida, a bioweapon
587 surrogate. Proc. Natl. Acad. Sci. U. S. A. *104*, 1009–1014.
588 https://doi.org/10.1073/pnas.0606713104.

589 57. Surette, M.G., and Bassler, B.L. (1998). Quorum sensing in Escherichia coli and
590 Salmonella typhimurium. Proc. Natl. Acad. Sci. U. S. A. *95*, 7046–7050.
591 https://doi.org/10.1073/pnas.95.12.7046.

592 58. van Hoek, M.L., Hoang, K.V., and Gunn, J.S. (2019). Two-Component Systems in
593 Francisella Species. Front. Cell. Infect. Microbiol. *9*, 198.
594 https://doi.org/10.3389/fcimb.2019.00198.

595 59. Lindgren, H., Shen, H., Zingmark, C., Golovliov, I., Conlan, W., and Sjöstedt, A.
596 (2007). Resistance of Francisella tularensis strains against reactive nitrogen and oxygen species
597 with special reference to the role of KatG. Infect. Immun. *75*, 1303–1309.
598 https://doi.org/10.1128/IAI.01717-06.

599 60. Brodmann, M., Dreier, R.F., Broz, P., and Basler, M. (2017). Francisella requires
600 dynamic type VI secretion system and ClpB to deliver effectors for phagosomal escape. Nat.
601 Commun. *8*, 15853. https://doi.org/10.1038/ncomms15853.

602 61. Brodmann, M., Heilig, R., Broz, P., and Basler, M. (2018). Mobilizable Plasmids for
603 Tunable Gene Expression in Francisella novicida. Front. Cell. Infect. Microbiol. *8*.
604 https://doi.org/10.3389/fcimb.2018.00284.

605 62. Harms, A., Segers, F.H.I.D., Quebatte, M., Mistl, C., Manfredi, P., Körner, J., Chomel,
606 B.B., Kosoy, M., Maruyama, S., Engel, P., et al. (2017). Evolutionary Dynamics of
607 Pathoadaptation Revealed by Three Independent Acquisitions of the VirB/D4 Type IV
608 Secretion System in Bartonella. Genome Biol. Evol. *9*, 761–776.
609 https://doi.org/10.1093/gbe/evx042.

610 63. Schindelin, J., Arganda-Carreras, I., Frise, E., Kaynig, V., Longair, M., Pietzsch, T.,
611 Preibisch, S., Rueden, C., Saalfeld, S., Schmid, B., et al. (2012). Fiji: an open-source platform
612 for biological-image analysis. Nat. Methods *9*, 676–682. https://doi.org/10.1038/nmeth.2019.

613 64. Aranda, P.S., LaJoie, D.M., and Jorcyk, C.L. (2012). Bleach gel: a simple agarose gel
614 for analyzing RNA quality. Electrophoresis *33*, 366–369.
615 https://doi.org/10.1002/elps.201100335.

616 65. Rohmer, L., Fong, C., Abmayr, S., Wasnick, M., Larson Freeman, T.J., Radey, M.,
617 Guina, T., Svensson, K., Hayden, H.S., Jacobs, M., et al. (2007). Comparison of Francisella
618 tularensis genomes reveals evolutionary events associated with the emergence of human
619 pathogenic strains. Genome Biol. *8*, R102. https://doi.org/10.1186/gb-2007-8-6-r102.

620 66. Magoc, T., Wood, D., and Salzberg, S.L. (2013). EDGE-pro: Estimated Degree of Gene
621 Expression in Prokaryotic Genomes. Evol. Bioinforma. Online *9*, 127–136.
622 https://doi.org/10.4137/EBO.S11250.

623 67. Love, M.I., Huber, W., and Anders, S. (2014). Moderated estimation of fold change and
624 dispersion for RNA-seq data with DESeq2. Genome Biol. *15*, 550.
625 https://doi.org/10.1186/s13059-014-0550-8.

626 68. Llewellyn, A.C., Jones, C.L., Napier, B.A., Bina, J.E., and Weiss, D.S. (2011).
627 Macrophage replication screen identifies a novel Francisella hydroperoxide resistance protein
628 involved in virulence. PloS One *6*, e24201. https://doi.org/10.1371/journal.pone.0024201.

629 69. Chaparian, R.R., and van Kessel, J.C. (2021). Promoter Pull-Down Assay: A
630 Biochemical Screen for DNA-Binding Proteins. Methods Mol. Biol. Clifton NJ *2346*, 165–172.
631 https://doi.org/10.1007/7651_2020_307.

632 70. Jutras, B.L., Verma, A., and Stevenson, B. (2012). Identification of novel DNA-binding
633 proteins using DNA-affinity chromatography/pull down. Curr. Protoc. Microbiol. *Chapter 1*,
634 Unit1F.1. https://doi.org/10.1002/9780471729259.mc01f01s24.

71. van Kempen, M., Kim, S.S., Tumescheit, C., Mirdita, M., Lee, J., Gilchrist, C.L.M., Söding, J., and Steinegger, M. (2023). Fast and accurate protein structure search with Foldseek. Nat. Biotechnol., 1–4. https://doi.org/10.1038/s41587-023-01773-0.

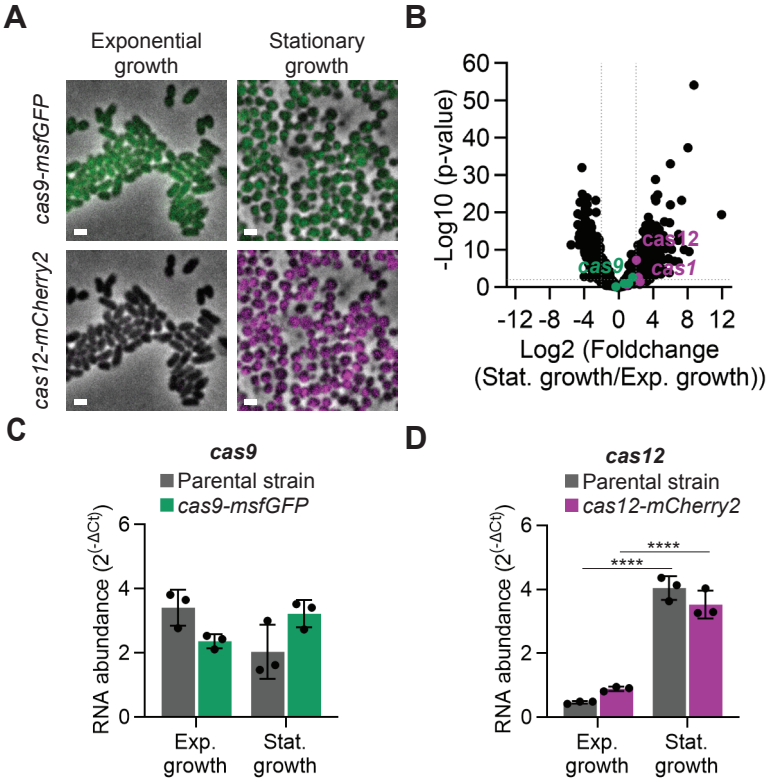

Figure 1
CRISPR nucleases Cas9 and Cas 12 are differentially expressed during exponential and stationary growth.
(A) Fluorescence microscopy of *cas9-msfGFP* and *cas12-mCherry2*. Fields of view of 13 x 13 µm are shown. Upper panel is a merge of phase contrast and GFP channel, lower panel is a merge of phase contrast and RFP channel. Scale bars represent 1 µm.
(B) RNA-seq data of differentially expressed genes in stationary and exponential growth phase. Green: *type II-B CRISPR-Cas* genes. Magenta: *type V-A CRISPR-Cas* genes. Dotted horizontal line: *P*-value of 0.01. Dotted vertical line: 4-fold difference.
(C-D) Determination of mRNA levels for *cas9* **(C)** and *cas12* **(D)** by RT-qPCR. Grey bars: Parental strain. Mean with standard deviation is displayed. Green bars: *cas9-msfGFP*. Magenta bars: *cas12-mCherry2*. Significant differences were determined with Tukey's multiple comparison test. **** *AdjP*-value < 0.0001.

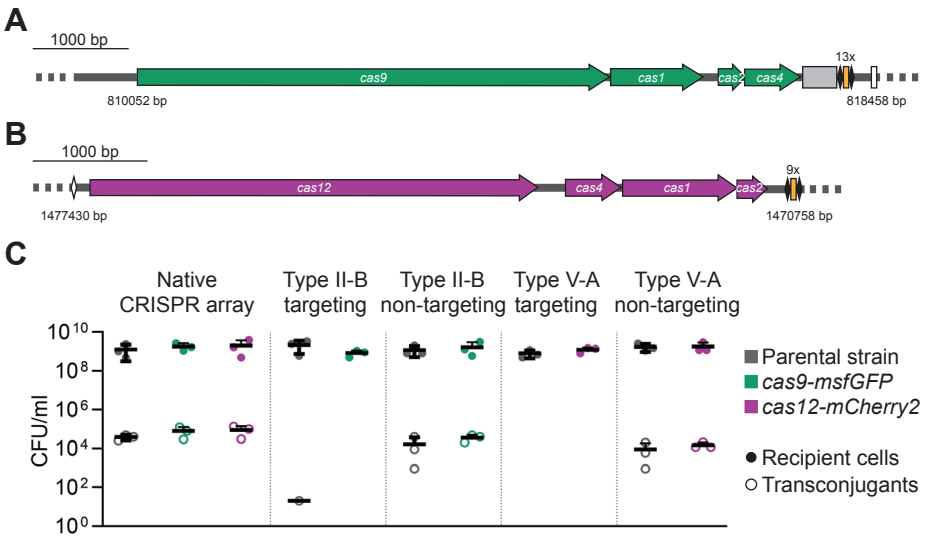

Supplemental figure 1
C-terminal fluorescent tags do not inhibit Cas9- and Cas12-mediated plasmid targeting.
(A) Type II-B CRISPR-Cas system in *F. novicida U112*. Green arrows: *cas* genes. Grey box: l*eader/tracr sequence*. Black diamonds: *repeats*. Orange box: *spacers*. White box: *scaRNA*. Drawn in scale.
(B) Type V-A CRISPR-Cas system in *F. novicida U112*. White diamond: *single repeat unit*. Magenta arrows: *cas* genes. Black diamonds: *repeats*. Orange box: *spacers*. Drawn in scale.
(C) Assessment of interference capability of wildtype and C-terminal tagged Cas9 and Cas12 in a conjugation-based plasmid inhibition assay. Strains have either both native type II-B and type V-A CRISPR arrays or have either CRISPR array replaced by a spacer matching a protospacer on the conjugated plasmid (targeting spacer) or one that does not match (non-targeting spacer). Mean with standard deviation is displayed. Filled circles: total number of cells. Empty circles: transformants. Grey circles: Parental strain. Green circles: *cas9-msfGFP*. Magenta circles: *cas12-mCherry2*.

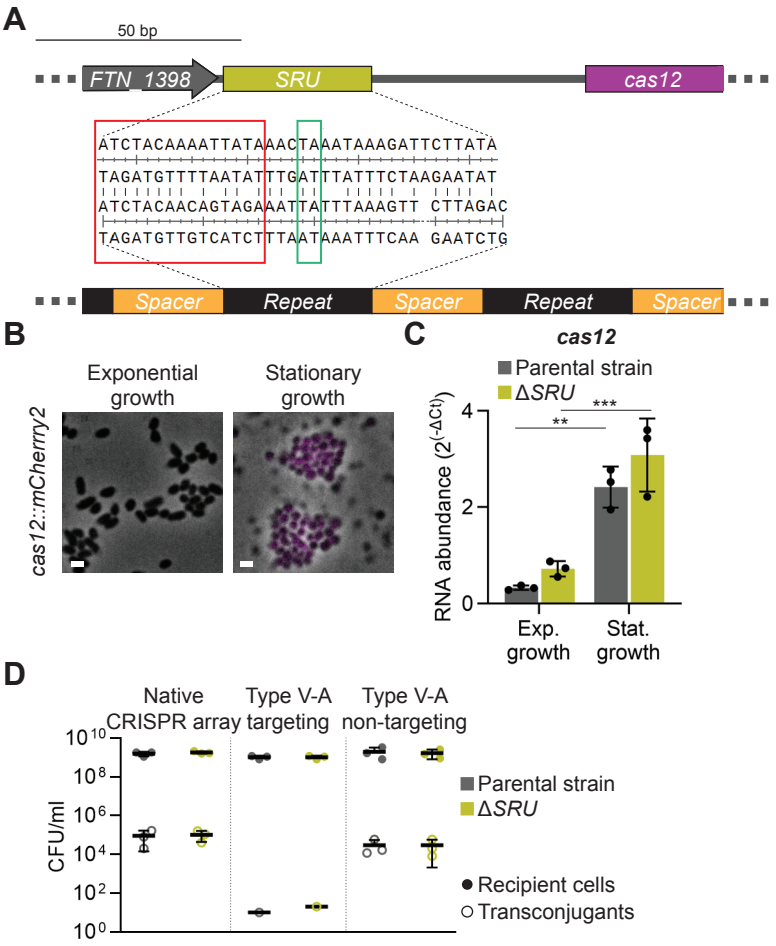

Figure 2

Cas12 and SRU are not involved in regulating *cas12* in stationary phase.

(A) CRISPR-like single repeat unit (SRU) is partially homologous to the type V-A CRISPR repeats. Red box: CRISPR-repeat stem loop; green box: cleavage site of Cas12 during pre-crRNA processing.

(B) Fluorescence microscopy of *cas12::mCherry2*. A merge of phase contrast and RFP channel in 13 x 13 µm fields of view are shown. Scale bars represent 1 µm.

(C) Determination of mRNA levels for *cas12* by RT-qPCR. Grey bars: Parental strain. Olive bars: Δ*SRU* mutant. Mean with standard deviation. Significant differences were determined with Tukey's multiple comparison test. ** *AdjP*-value < 0.005, *** *AdjP*-value < 0.001.

(D) Assessment of interference capability of parental strain and a Δ*SRU* mutant in a conjugation-based plasmid inhibition assay. Strains have either a native type V-A CRISPR array or have the CRISPR array replaced by a spacer matching a protospacer on the conjugated plasmid (targeting spacer) or one that does not match (non-targeting spacer). Mean with standard deviation is displayed. Filled circles: total number of cells. Empty circles: transformants. Grey circles: Parental strain. Olive circles: Δ*SRU* mutant.

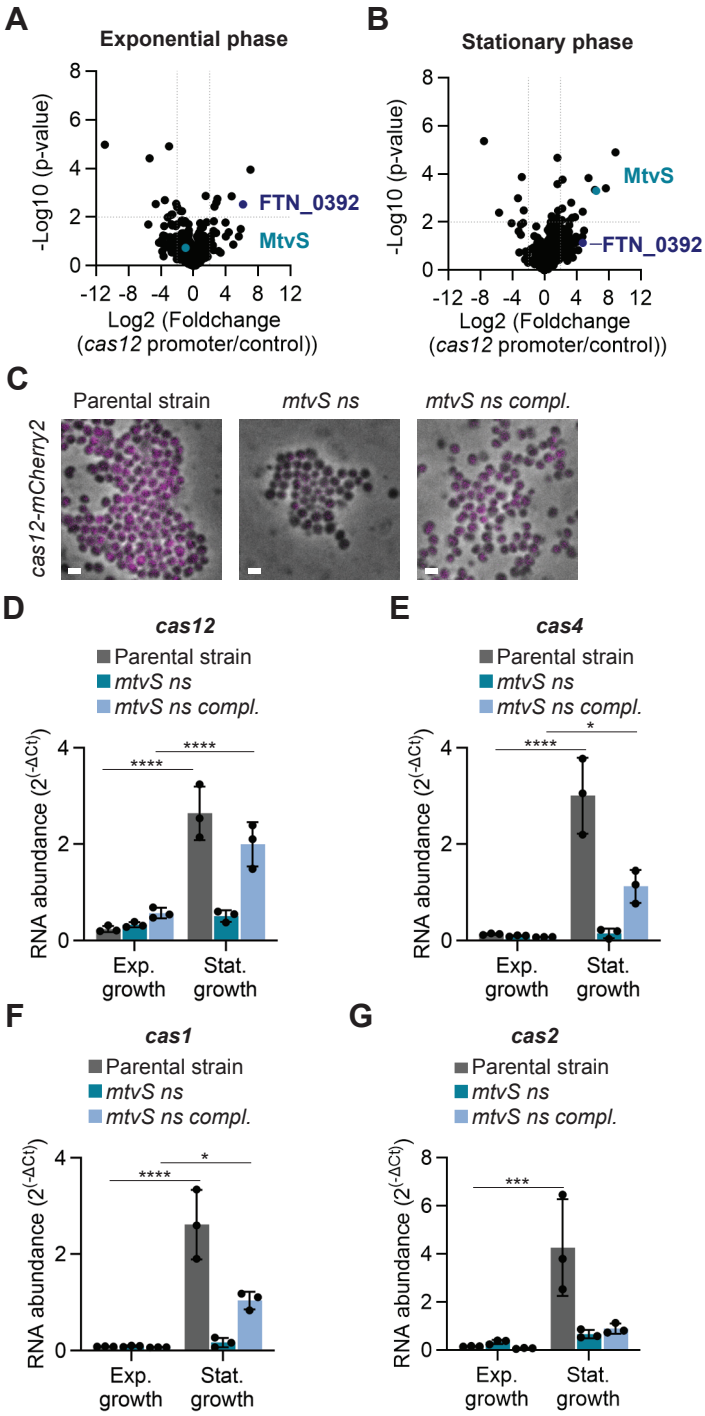

Figure 3

MtvS modulates expression of the Type V-A CRISPR-Cas system in *F. novicida* U112.

(A) Pull-down of proteins from exponential growth phase lysate binding specifically to the *cas12* promoter DNA sequence. Turquoise circle: MtvS. Dark blue circle: FTN_0392. Dotted horizontal line: *P*-value of 0.01. Dotted vertical line: 4-fold difference.

(B) Pull-down of proteins from stationary phase lysate binding specifically to the *cas12* promoter DNA sequence. Turquoise circle: MtvS. Dark blue circle: FTN_0392. Dotted horizontal line: *P*-value of 0.01. Dotted vertical line: 4-fold difference.

(C) Fluorescence microscopy of *cas12-mCherry2* in parental strain, *mtvS nonsense* mutant and *mtvS nonsense* mutant with wild-type *mtvS* at Tn7 insertion site. *mtvS nonsense* mutant results in decreased fluorescence intensity in stationary phase compared to parental strain and rescued mutant. Merge of phase contrast and RFP channel in 13 x 13 µm fields of view are shown. Scale bars represent 1 µm.

(D-G) Determination of mRNA levels for *cas12* **(C)** *cas4* **(D)**, *cas1* **(E)** and *cas2* **(F)** by RT-qPCR. Grey bars: Parental strain. Turquoise bars: *mtvS nonsense* mutant. Light blue bars: *mtvS nonsense* mutant with wild-type *mtvS* at Tn7 insertion site. Mean with standard deviation is displayed. Significant differences were determined with Tukey's multiple comparison test. * *AdjP*-value < 0.05, *** *AdjP*-value < 0.001, **** *AdjP*-value < 0.0001.

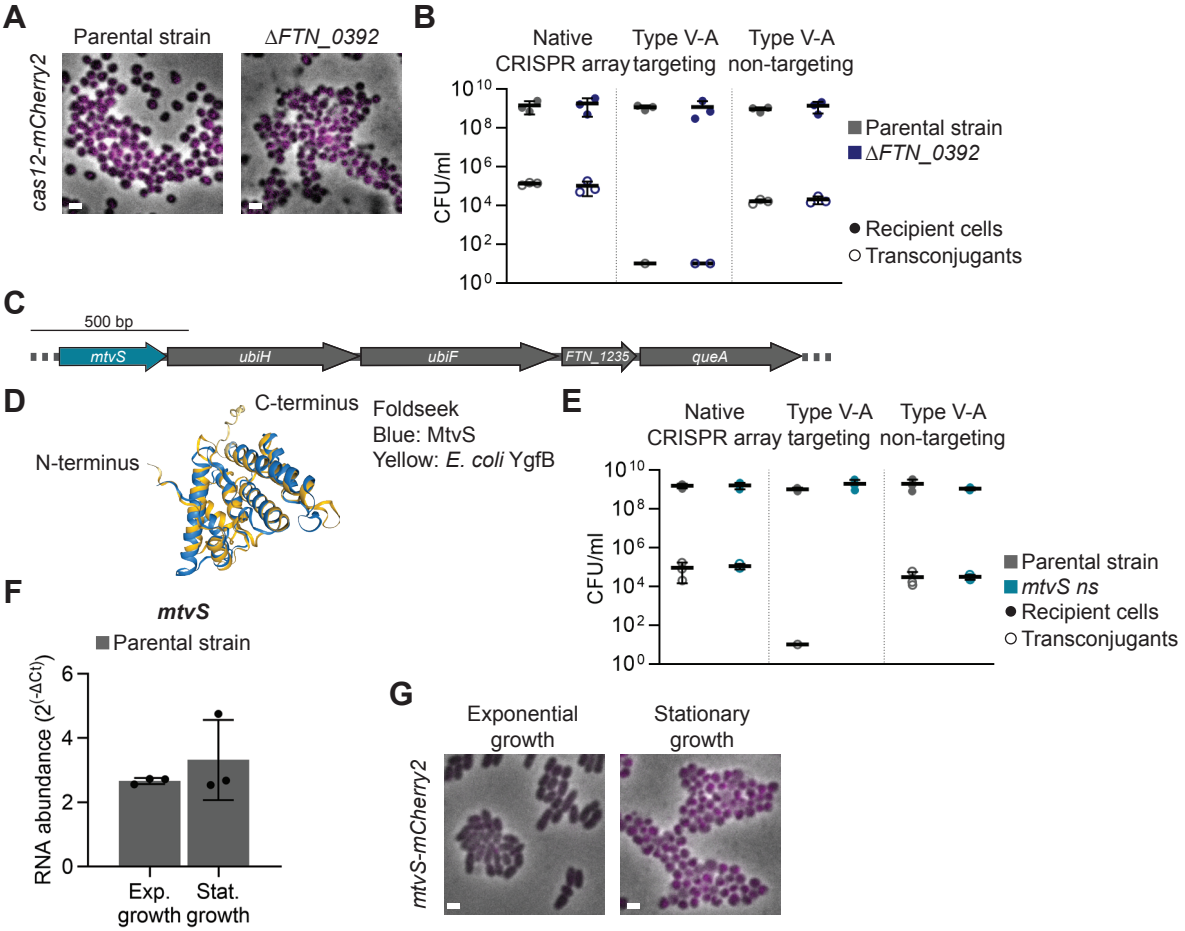

Supplemental figure 2
MtvS is a YgfB/YecA-like protein.
(A) Fluorescence microscopy of *cas12-mCherry2* in parental strain and Δ*FTN_0392* mutant. Comparable fluorescent intensities in stationary growth were detected. Merge of phase contrast and RFP channel in 13 x 13 µm fields of view are shown. Scale bars represent 1 µm.
(B) Assessment of interference capability of parental strain and Δ*FTN_0392* mutant in a conjugation-based plasmid inhibition assay. Strains have either a native type V-A CRISPR array or have the CRISPR array replaced by a spacer matching a protospacer on the conjugated plasmid (targeting spacer) or one that does not match (non-targeting spacer). Mean with standard deviation is displayed. Filled circles: total number of cells. Empty circles: transformants. Grey circles: Parental strain. Dark blue circles: Δ*FTN_0392* mutant.
(C) *mtvS* is the first gene of a conserved operon which also includes *ubiH* (2-octaprenyl-6-methoxyphenyl hydroxylase), *ubiF* (2-octaprenyl-3-methyl-6-methoxy-1,4-benzoquinol hydroxylase), *FTN_1235* (putative phage protein) and *queA* (S-adenosylmethionine:tRNA ribosyltransferase-isomerase).
(D) Comparison of Alphafold MtvS structure (blue) with *E. coli* YecA (yellow) by Foldseek.
(E) Assessment of interference capability of parental strain and *mtvS nonsense* mutant in a conjugation-based plasmid inhibition assay. Strains have either a native type V-A CRISPR array or have the CRISPR array replaced by a spacer matching a protospacer on the conjugated plasmid (targeting spacer) or one that does not match (non-targeting spacer). Mean with standard deviation is displayed. Filled circles: total number of cells. Empty circles: transformants. Grey circles: Parental strain. Turquoise circles: *mtvS nonsense* mutant.
(F) Fluorescence microscopy of *mtvS-mCherry2* in parental strain. Fluorescence intensity is higher in stationary phase than in exponential growth phase. Merge of phase contrast and RFP channel in 13 x 13 µm fields of view are shown. Scale bars represent 1 µm.
(G) Determination of mRNA levels for *mtvS* in the parental strain by RT-qPCR. Grey bars: Parental strain. Mean with standard deviation is displayed. Significant differences were determined with Tukey's multiple comparison test.

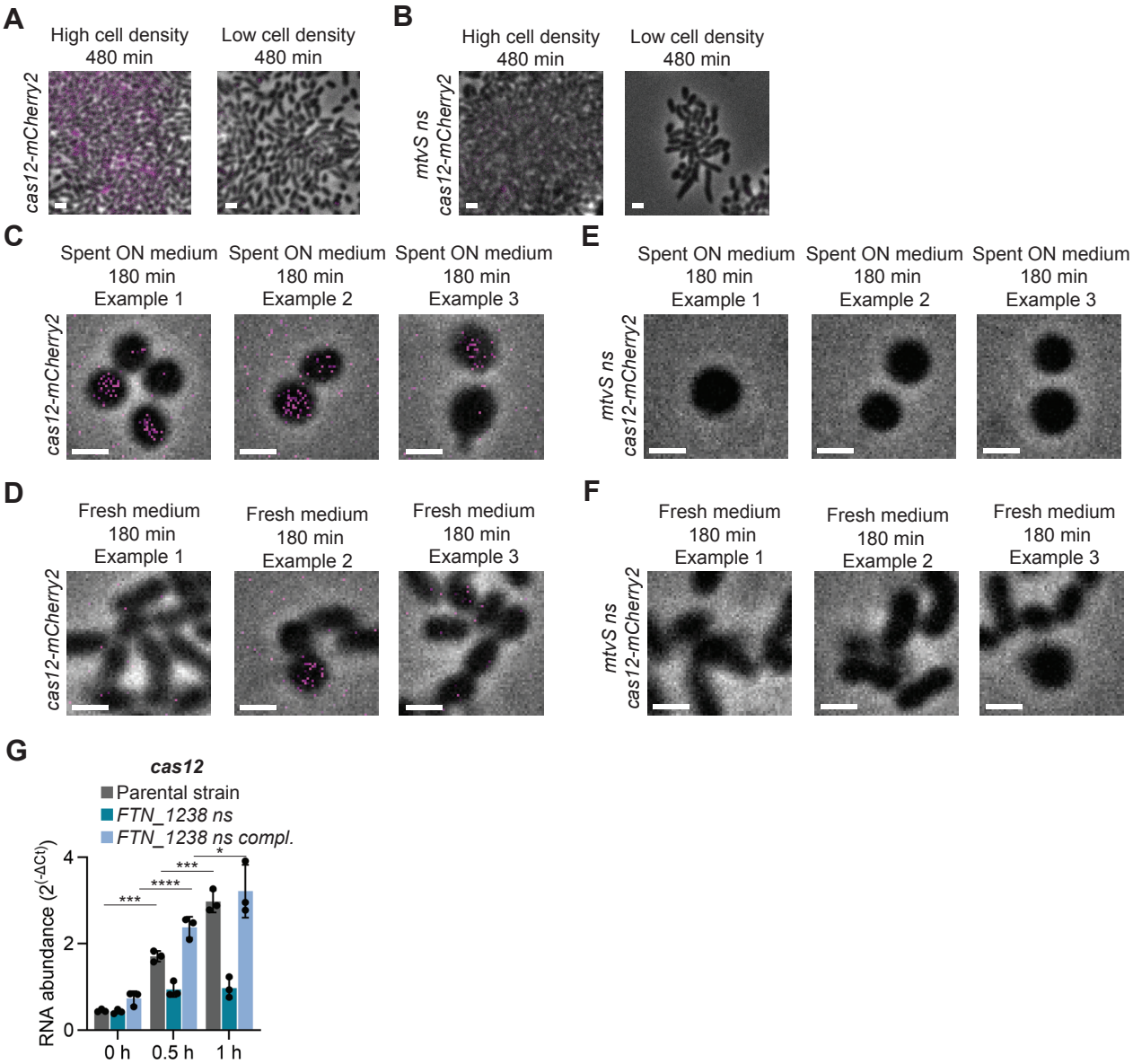

Figure 4

MtvS modulates *cas12* expression in a cell-density dependent manner

(A) Fluorescence microscopy of *cas12-mCherry2* in microfluidic plate. BHI was flown through for 8 h. Merge of phase contrast and RFP channel in 13 x 13 µm fields of view are shown. Same contrast settings as in **(B)**. Scale bars represent 1 µm.

(B) Fluorescence microscopy of *cas12-mCherry2* in *mtvS nonsense* mutant in microfluidic plate. BHI was flown through for 8 h. Merge of phase contrast and RFP channel in 13 x 13 µm fields of view are shown. Same contrast settings as in (**A**). Scale bars represent 1 µm.

(C-D) Fluorescence microscopy of *cas12-mCherry2* in microfluidic plate. BHI was flown through for 1 h before switching to spent overnight medium of parental strain for 4h. Afterwards, fresh BHI was flown through for 3 h. **(C)** Three examples of 240 min time point (180 min after switching to spent ON medium) and **(D)** three examples of 480 min (180 min after switching back to fresh BHI) are shown. Merge of phase contrast and RFP channel in 4 x 4 µm fields of view are shown. Same contrast settings as in (**E-F)** and **supplemental figure 3 (A)**. Scale bars represent 1 µm.

(E-F) Fluorescence microscopy of *cas12-mCherry2* in *mtvS nonsense* mutant in microfluidic plate. BHI was flown through for 1 h before switching to spent overnight medium of parental strain for 4h. Afterwards, fresh BHI was flown through for 3 h. **(E)** Three examples of 240 min time point (180 min after switching to spent ON medium) and **(F)** three examples of 480 min (180 min after switching back to fresh BHI) are shownare shown. Merge of phase contrast and RFP channel in 4 x 4 µm fields of view are shown. Same contrast settings as in (**C-D)** and **supplemental figure 3 (A)** . Scale bars represent 1 µm.

(G) Determination of mRNA levels for *cas12* after switching to spent overnight medium by RT-qPCR. Samples were taken 0 h, 0.5 h and 1 h after medium change. Grey bars: Parental strain. Turquoise bars: *mtvS nonsense* mutant. Light blue bars: *mtvS nonsense* mutant with wild-type *mtvS* at Tn7 insertion site. Mean with standard deviation is displayed. Significant differences were determined with Tukey's multiple comparison test. * *AdjP*-value < 0.05, *** *AdjP*-value < 0.001, **** *AdjP*-value < 0.0001.

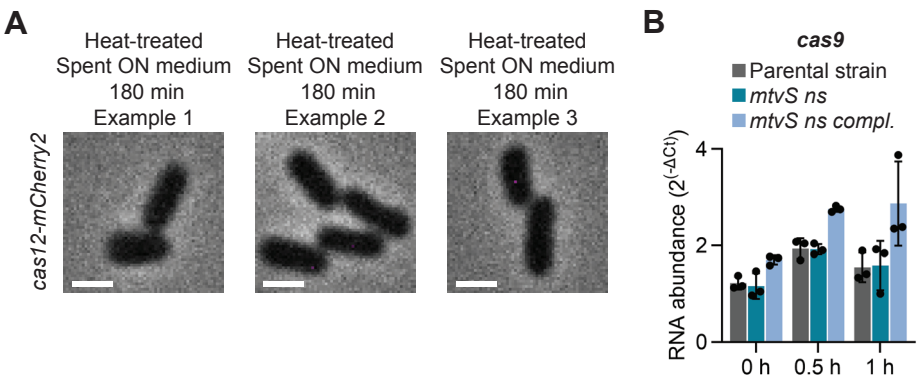

Supplement figure 3

Spent overnight medium is heat sensitive and does not affect *cas9* expression.

(A) Fluorescence microscopy of *cas12-mCherry2* in microfluidic plate. BHI was flown through for 1 h before switching to heat-treated spent overnight medium of parental strain for 4h. Afterwards fresh BHI was flown through for 3 h. Three examples of 240 min time point (180 min after switching to spent ON medium) are shown. Merge of phase contrast and RFP channel in 4 x 4 µm fields of view are shown. Same contrast settings as in Figs. **3 (C-F)**. Scale bars represent 1 µm.

(B) Determination of mRNA levels for *cas9* after switching to spent overnight medium by RT-qPCR. Samples were taken 0 h, 0.5 h and 1 h after medium change. Grey bars: Parental strain. Turquoise bars: *mtvS nonsense* mutant. Light blue bars: *mtvS nonsense* mutant with wild-type *mtvS* at Tn7 insertion site. Mean with standard deviation is displayed. Significant differences were determined with Tukey's multiple comparison test.

Table 1: Strains used in this study, related to Material and methods

Organism	Genotype	Plasmid	Relevant features	Source
Francisella novicida U112			Parental strain	Bei resources (NR-13)
	typeII_tet_spacer_targ		Type II-B wild-type CRISPR array was replaced with targeting spacer matching *tetR* on plasmid pFNMB2	This study
	typeII_tet_spacer_nontarg		Type II-B wild-type CRISPR array was replaced with non-targeting spacer matching *tetR* on plasmid pFNMB2	This study
	typeV_tet_spacer_targ		Type V-A wild-type CRISPR array was replaced with targeting spacer matching *tetR* on plasmid pFNMB2	This study
	typeV_tet_spacer_nontarg		Type V-A wild-type CRISPR array was replaced with non-targeting spacer matching *tetR* on plasmid pFNMB2	This study
	mtvS nonsense		Three stop codons introduced at position 11 of *mtvs*	This study
	mtvS nonsense, *Tn7_mtvS*		Wild-type *mtvS* was introduced at the canonical Tn7 insertion site downstream of *glmS*	This study
	mtvS nonsense, *typeV_tet_spacer_targ*		Type V-A wild-type CRISPR array was replaced with targeting spacer matching *tetR* on plasmid pFNMB2	This study
	mtvs nonsense, *typeV_tet_spacer_nontarg*		Type V-A wild-type CRISPR array was replaced with non-targeting spacer matching *tetR* on plasmid pFNMB2	This study
	Δ*SRU*		Deletion of single repeat unit (SRU) in *cas12* promoter	This study
	Δ*SRU*, *typeV_tet_spacer_targ*		Type V-A wild-type CRISPR array was replaced with targeting spacer matching *tetR* on plasmid pFNMB2	This study
	Δ*SRU*, *typeV_tet_spacer_nontarg*		Type V-A wild-type CRISPR array was replaced with non-targeting spacer matching *tetR* on plasmid pFNMB2	This study
	ΔFTN_0392		Deletion of FTN_0392	This study
	ΔFTN_0392, *typeV_tet_spacer_targ*		Type V-A wild-type CRISPR array was replaced with targeting spacer matching *tetR* on plasmid pFNMB2	This study
	ΔFTN_0392, *typeV_tet_spacer_nontarg*		Type V-A wild-type CRISPR array was replaced with non-targeting spacer matching *tetR* on plasmid pFNMB2	This study
	cas9-msfGFP, *cas12-mCherry2*		C-terminal chromosomal fusion of *msfgfp* to *cas9* and c-terminal chromosomal fusion of *mCherry2* to *cas12*	This study
	cas9-msfGFP, *cas12-mCherry2*, *typeV_tet_spacer_targ*		Type V-A wild-type CRISPR array replaced with targeting spacer matching *tetR* on plasmid pFNMB2	This study
	cas9-msfGFP, *cas12-mCherry2*, *typeV_tet_spacer_nontarg*		Type V-A wild-type CRISPR array replaced with non-targeting spacer matching *tetR* on plasmid pFNMB2	This study
	cas9-msfGFP, *cas12-mCherry2*, *typeII_tet_spacer_targ*		Type II-B wild-type CRISPR array replaced with targeting spacer matching *tetR* on plasmid pFNMB2	This study
	cas9-msfGFP, *cas12-mCherry2*, *typeII_tet_spacer_nontarg*		Type II-B wild-type CRISPR array replaced with non-targeting spacer matching *tetR* on plasmid pFNMB2	This study
	cas9-msfGFP, *cas12-mCherry2*, *mtvs nonsense*		Three stop codons introduced at position 11 of *mtvS*	This study
	cas12::mCherry2		*cas12* was replaced with *mCherry2*	This study
Escherichia coli OneShotpir			Cloning strain	ThermoFisher
Escherichia coli JKE 201			Donor *E. coli* used for conjugation into *F. novicida*	[1]
		pFNMB2 *msfGFP*	Donor *E. coli* containing mobilizable *Francisella* plasmid pFNMB2 *msfGFP*	[2]

Table 2: Plasmids and primers used to generate mutants, related to Material and Methods.

Plasmid Name	Spacer/Peptide sequence	Primers	Sequence 5'-3' [base pairs]
pDMK3 *typeII_tet_spacer_targ*	TCGCGATGACTTAGTAAAGCACATC TAAAACTTT	TypeII_spacer_1.FOR	CTGAATTGTCGACCCTCGAGATAGTTGACTGGGTTATAG
		TypeII_spacer_tet_targ_1.REV	AAAGTTTTAGATGTGCTTTACTAAGTCATCGCGAGTTTCAGTTGCTGAATTAT TTGGTAAACTACTGTTAGAGCCAAAACAAACCTAGTGT
		TypeII_spacer_tet_targ_2.FOR	TCGCGATGACTTAGTAAAGCACATCTAAAACTTTCTAACAGTAGTTTACCAA ATAATTCAGCAACTGAAACTTAATTAATTTTGTAAATTA
		TypeII_spacer_2.REV	ATCTATCTAGAAGGGCCCCGTTTCACTAAATTCTTA
		TypeII_spacer_Det.FOR	ATGGGTTGCTCAAGGTGAAG
		TypeII_spacer_Det.REV	TCTCATGCTGGTTACGCTTG
pDMK3 *typeII_tet_spacer_nontarg*	AAAGTTTTAGATGTGCTTTACTAAG TCATCGCGA	TypeII_spacer_1.FOR	CTGAATTGTCGACCCTCGAGATAGTTGACTGGGTTATAG
		TypeII_spacer_tet_nontarg_1.REV	TCGCGATGACTTAGTAAAGCACATCTAAAACTTTGTTTCAGTTGCTGAATTA TTTGGTAAACTACTGTTAGAGCCAAAACAAACCTAGTGT
		TypeII_spacer_tet_nontarg_2.FOR	AAAGTTTTAGATGTGCTTTACTAAGTCATCGCGACTAACAGTAGTTTACCAA ATAATTCAGCAACTGAAACTTAATTAATTTTGTAAATTA
		TypeII_spacer_2.REV	ATCTATCTAGAAGGGCCCCGTTTCACTAAATTCTTA
		TypeII_spacer_Det.FOR	ATGGGTTGCTCAAGGTGAAG
		TypeII_spacer_Det.REV	TCTCATGCTGGTTACGCTTG
pDMK3 *typeV_tet_spacer_targ*	TCTAACATCTCAATGGCTAAGGCGT CGAG	TypeV_spacer_1.FOR	TCTATCGCCTTCTTGACGAGTTCTTCTGAATTGTCGACCCTCGAGATGCTGTT TCCAAGC
		TypeV_spacer_tet_targ_1.REV	CTCGACGCCTTAGCCATTGAGATGTTAGAGTCTAAGAACTTTAAATAATTTG TCTGTATATTATTGATTTCTAAATTAGAATTTT
		TypeV_spacer_tet_targ_2.FOR	TCTAACATCTCAATGGCTAAGGCGTCGAGATCTACAACAGTAGAAATTATTT AAAGTTCTTAGACCCGTTTTTGCCTAAATCAGC
		TypeV_spacer_2.REV	TTGTGAGCGGATAACAATTTGTGGAATTCCCGGGAGAGCTCCCTAGTTTGTG ACTTTGTT
		TypeV_spacer_Det.FOR	GCCAGCGAATAAAAGTCCTG
		TypeV_spacer_Det.REV	CAAGCCTAGCGGAGCTAATG
pDMK3 *typeV_tet_spacer_nontarg*	CTCGACGCCTTAGCCATTGAGATGT TAGA	TypeV_spacer_1.FOR	TCTATCGCCTTCTTGACGAGTTCTTCTGAATTGTCGACCCTCGAGATGCTGTT TCCAAGC
		TypeV_spacer_tet_nontarg_1.REV	TCTAACATCTCAATGGCTAAGGCGTCGAGGTCTAAGAACTTTAAATAATTTG TCTGTATATTATTGATTTCTAAATTAGAATTTT
		TypeV_spacer_tet_nontarg_2.FOR	CTCGACGCCTTAGCCATTGAGATGTTAGAATCTACAACAGTAGAAATTATTT AAAGTTCTTAGACCCGTTTTTGCCTAAATCAGC
		TypeV_spacer_2.REV	TTGTGAGCGGATAACAATTTGTGGAATTCCCGGGAGAGCTCCCTAGTTTGTG ACTTTGTT
		TypeV_spacer_Det.FOR	GCCAGCGAATAAAAGTCCTG
		TypeV_spacer_Det.REV	CAAGCCTAGCGGAGCTAATG
pDMK3 *mtvS nonsense*	MVKLA***DEFNP	FTN_1238_ns_1.FOR	CTTCTGAATTGTCGACCCTCGAGCCAAATAAGCCTACTCCT
		FTN_1238_ ns_1.REV	AGATTAGTAGTAGGCATTAAAAGTAATGCAA
		FTN_1238_ns_2.FOR	TACTTTTAATGCCTACTACTAATCTTCAAAATTAGGTTTTT
		FTN_1238_ns_2.REV	ATAACAATTTGTGGAATTCCCGGGAGAGCTCAGGTTACGCGGCCGCCCACCC ATGCCCATT
		FTN_1238_ns_Det.FOR	CCAACTATCCCACCCCCAAC

		FTN_1238_ns_Det.REV	TTTGCTGCTCATCAAAGGCT
		FTN_1238_ns_Det2.FOR	CCTACTACTAATCTTCAAAATTAG
pDMK3 *Tn7_mtvS*		FTN_0485_Tn7_1.FOR	CTTCTGAATTGTCGACCCTCGAGAATGTGCCAAATAGTTCG
		FTN_1238_Tn7_1.REV	TTTAGGTATTAACTTGGAAAATAAATGATAAGAAAGTAAAA
		FTN_1238_Tn7_2.FOR	TTTATTTTCCAAGTTAATACCTAAATTTTTTCACTAT
		FTN_1238_Tn7_2.REV	ATTTAGCTAAGTTTAAACTCTTGATTACATAGCC
		FTN_1238_Tn7_3.FOR	ATCAAGAGTTTAAACTTAGCTAAATCTGTAACC
		FTN_0485_Tn7_3.REV	AGAGCTCAGGTTACGCGGCCGCGTATCAAGCAAGAGCTTAG
		FTN_0485_Tn7_Det.FOR	TCGTTGCATGTGGAACTAGCT
		FTN_0485_Tn7_Det.REV	TGGTGAAACACTAGCTGAAGGT
pDMK3 Δ*SRU*	Deleted: TATTATAAGAATCTTTATTTAGTTTATAATTTTGTAGAT	dSRU_1.FOR	CTTCTGAATTGTCGACCCTCGAGAATTTGTTCATAGTTTATAGCTT
		dSRU_1.REV	CAAAATTTTTTAGACTTTATATATAATCGAAATGTAGAG
		dSRU_2.FOR	TATATATAAAGTCTAAAAAATTTTGCCAAACTCA
		dSRU_2.REV	AGAGCTCAGGTTACGCGGCCGCATTTTGATAAAGGTAAAAGAGC
		dSRU_Det.FOR	ACCGCTGTACCAATAACACTAT
		dSRU_Det.REV	ACACTTGCTGATGTTGGTGA
pDMK3 Δ*FTN_0392*	MRITLKQLQVFIEKDINGCDIRLENFSI*	dFTN_0392_1.FOR	TCTATCGCCTTCTTGACGAGTTCTTCTGAATTGTCGACCCTCGAGAAGTGTTCTTACGTACA
		dFTN_0392_1.REV	CTCTAAAACAGCTTCAAGTGTTTATAGAGAAAGATATAAATGGCTG
		dFTN_0392_2.FOR	TTTATATCTTTCTCTATAAACACTTGAAGCTGTTT
		dFTN_0392_2.REV	ATAACAATTTGTGGAATTCCCGGGAGAGCTCAGGTTACGCGGCCGCGTGAGACGAACCAAAAAC
		dFTN_0392_Det.FOR	TGCAAATTCACTATAGCGCCA
		dFTN_0392_Det.REV	TTGCAACATCCTCAACCCCA
pDMK3 *cas9-msfGFP*		FTN_0757-fusion_1.FOR	ATTGTCGACCCTCGAGCAAGCAGGTTTTGGATAAG
		FTN_0757-fusion_1.REV	GCGGCCGCATTATTAGATGTTTCATTATAAATACCT
		FTN_0757-fusion_2.FOR	TCTAATAATGCGGCCGCAGGA
		FTN_0757-msfGFP_2.REV	TACCAAGCATTTTGTAGAGCTCATCCATG
		FTN_0757-msfGFP_3.FOR	GCTCTACAAAATGCTTGGTATGAAATTAG
		FTN_0757-fusion_3.REV	ACAATTTGTGGAATTCCCGGGCGATACTCCTCCATTAGA
		FTN_0757-fusion_Det.FOR	TCTAAAAACCCAAAAATTACATGAG
		FTN_0757-fusion_Det.REV	TGTTCACCAGCAAATTCTCCAG
pDMK3 *cas12-mCherry2*		FTN_1397-fusion_1.FOR	CTGAATTGTCGACCCTCGAGCAAAAATATTAACAAAAACTATATTCTTT
		FTN_1397-mCherry2_1.REV	TGTACAAGTTATTTGAGTTCGTGCAGA
		FTN_1397-mCherry2_2.FOR	ACGAACTCAAATAACTTGTACAGCTCGT
		FTN_1397-fusion_2.REV	GAATAACGCGGCCGCAGGA
		FTN_1397-fusion_3.FOR	CGGCCGCGTTATTCCTATTCTGCACG
		FTN_1397-fusion_3.REV	CAATTTGTGGAATTCCCGGGGTGCTTAGAGCTTATCAG
		FTN_1397-fusion_Det.FOR	TCTCTTGCTGCTCTGGAGTT
		FTN_1397-fusion_Det.REV	AAAAGAGGGCGTTTCAAGGT
pDMK3 *cas12::mCherry2*		FTN_1397::mCherry2_1.FOR	CTTCTGAATTGTCGACCCTCGAGAGTCCGTTTTATCACATAAG
		FTN_1397::mCherry2_1.REV	TGTACAAGTAAGGTAGGATCAAAAATAATCA
		FTN_1397::mCherry2_2.FOR	TGATCCTACCTTACTTGTACAGCTCGTC
		FTN_1397::mCherry2_2.REV	AGTCTTTATCATGGTGAGCAAGGGC
		FTN_1397::mCherry2_3.FOR	GCTCACCATGATAAAGACTCCTTATAAAATT
		FTN_1397::mCherry2_3.REV	TCAGTAGCGGCCGCATTTTGATAAAGGTAAAAGAGC

	FTN_1397::mCherry2_Det.FOR	TCTCTTGCTGCTCTGGAGTT
	FTN_1397::mCherry2_Det.REV	ACACTTGCTGATGTTGGTGA

Table 3: Primers used for RT-qPCR, related to Material and methods.

Primers	Sequence 5'-3' [base pairs]
FTN_0757_qPCR. FOR	ATGCTAACACTTGTGCAGTTTG
FTN_0757_qPCR.REV	GTCTCTGAGCTTTGGCACTTA
FTN_1397_qPCR.FOR	AAGCTCTGCCTCACCATTTAG
FTN_1397_qPCR.REV	AAGGGCGACCAAATCTACATAC
FTN_1396_qPCR.FOR	GCCCATCTCTTGGAGACAAA
FTN_1396_qPCR.REV	GGGCTTACTTGTGGAGAGAAA
FTN_1395_qPCR.FOR	TATTCTAGGTTTGCGCCCTTG
FTN_1395_qPCR.REV	CAAGCCTAGCGGAGCTAATG
FTN_1394_qPCR.FOR	TCACATCTTTATCTGGAGCATT
FTN_1394_qPCR.REV	TGGTGTACGTTTACAATATTCGG
FTN_1238_qPCR.FOR	CACCCTCTTCAATCGGCTTAG
FTN_1238_qPCR.REV	GGACTGCTTTGTGCTTTGTTT

Table 4: Primers used for promoter sequence pull-down

Primers	Modification	Sequence 5'-3' [base pairs]
Promoter-FTN_1397.FOR		CTAGCTAGTTTAAAAGGACAA
Promoter-FTN_1397_biotin.REV	5' Biotin-TEG	TAACTCAAATCTTAGAGTTTTACTT
FTN_1397_pull-down.FOR		GCTGTACCAATAACACTATAAT
FTN_1397_biotin.REV	5' Biotin-TEG	AGAAAAATCTATTAAAGAAACACTATC

Table 5: Sequencing and EDGE-Pro statistics. RPKM reads were calculated as "Mapped reads"- "rRNA reads" and were the basis to calculate RPKM values. Related to Results.

	Parental strain Exponential growth Replicate 1	**Parental strain Exponential growth Replicate 2**	**Parental strain Exponential growth Replicate 3**	**Parental strain Stationary phase Replicate 1**	**Parental strain Stationary phase Replicate 2**	**Parental strain Stationary phase Replicate 3**
Total reads	3724938	3843094	3742820	2405842	2339574	3527853
Mapped reads	3596390	3768817	3666864	2234312	2095603	3262475
Unique reads	2586825	3630328	3559936	2170528	1391360	2017405
Multiple reads	1009565	138489	106928	63784	704243	1245070
rRNA reads	950125	27813	1105	62713	701355	1241682
RPKM reads	2646265	3741004	3665759	2171599	1394248	2020793

References

1. Harms, A., Segers, F.H.I.D., Quebatte, M., Mistl, C., Manfredi, P., Körner, J., Chomel, B.B., Kosoy, M., Maruyama, S., Engel, P., et al. (2017). Evolutionary Dynamics of Pathoadaptation Revealed by Three Independent Acquisitions of the VirB/D4 Type IV Secretion System in *Bartonella*. Genome Biol. Evol. *9*, 761–776. https://doi.org/10.1093/gbe/evx042.

2. Brodmann, M., Heilig, R., Broz, P., and Basler, M. (2018). Mobilizable Plasmids for Tunable Gene Expression in *Francisella novicida.* Front. Cell. Infect. Microbiol. *8*. https://doi.org/10.3389/fcimb.2018.00284.